

Article

# Ru/Al<sub>2</sub>O<sub>3</sub> on Polymer-Derived SiC Foams as Structured Catalysts for CO<sub>2</sub> Methanation

Elisabetta Maria Cepollaro <sup>1,\*</sup>, Stefano Cimino <sup>1,\*</sup>, Luciana Lisi <sup>1</sup>, Mattia Biesuz <sup>2</sup>, Balanand Santhosh <sup>2</sup>  
and Gian Domenico Sorarù <sup>2,\*</sup>

<sup>1</sup> Istituto di Scienze e Tecnologie per l'Energia e la Mobilità Sostenibili (STEMS), Consiglio Nazionale delle Ricerche (CNR), Via Guglielmo Marconi 4/10, 80125 Napoli, Italy

<sup>2</sup> Dipartimento di Ingegneria Industriale, Università di Trento, Via Sommarive, 38123 Trento, Italy

\* Correspondence: stefano.cimino@cnr.it (S.C.); giandomenico.sorarù@unitn.it (G.D.S.)

**Abstract:** The catalytic methanation of CO<sub>2</sub> via the strongly exothermic equilibrium Sabatier reaction requires the development of structured catalysts with enhanced mass- and heat-transfer features to limit hot-spot formation, avoid catalyst deactivation, and control process selectivity. In this work, we investigated the use of polymer-derived SiC open-cell foams as structured carriers onto which  $\gamma$ -Al<sub>2</sub>O<sub>3</sub> was applied by either dip-coating or pore-filling methods; eventually, Ru was dispersed by impregnation. The formation of an undesired insulating SiO<sub>2</sub> layer on the surface of the SiC struts was prevented by a pyrolysis treatment under an inert atmosphere at temperatures varying from 800 up to 1800 °C. SiC foam substrates and their corresponding structured catalysts were characterized by SEM, XRD, N<sub>2</sub> physisorption, and compressive strength measurements, and their CO<sub>2</sub> methanation activity was tested at atmospheric pressure in a fixed bed flow reactor operated in the temperature range from 200 to 450 °C. SiC foams obtained at intermediate pyrolysis temperatures (1000–1200 °C) showed good mechanical strength and high compatibility with the Ru/Al<sub>2</sub>O<sub>3</sub> active catalytic overlayer.



**Citation:** Cepollaro, E.M.; Cimino, S.; Lisi, L.; Biesuz, M.; Santhosh, B.; Sorarù, G.D. Ru/Al<sub>2</sub>O<sub>3</sub> on Polymer-Derived SiC Foams as Structured Catalysts for CO<sub>2</sub> Methanation. *Catalysts* **2022**, *12*, 956. <https://doi.org/10.3390/catal12090956>

Academic Editor: Anastasia Macario

Received: 22 July 2022

Accepted: 23 August 2022

Published: 28 August 2022

**Publisher's Note:** MDPI stays neutral with regard to jurisdictional claims in published maps and institutional affiliations.



**Copyright:** © 2022 by the authors. Licensee MDPI, Basel, Switzerland. This article is an open access article distributed under the terms and conditions of the Creative Commons Attribution (CC BY) license (<https://creativecommons.org/licenses/by/4.0/>).

**Keywords:** CO<sub>2</sub> utilization; hydrogenation; structured catalysts; polymer-derived ceramics; open-cell foams; SiC; Ruthenium

## 1. Introduction

The increasing levels of CO<sub>2</sub> in the atmosphere and the consequential global warming effect demand the development of novel techniques for CO<sub>2</sub> capture. At the same time, the increasing use of intermittent renewable energy sources involves the physical or chemical storage of H<sub>2</sub>, which is over-produced in some conditions. To this end, the conversion of captured CO<sub>2</sub> into fuels such as methane (Power-to-Gas) through its hydrogenation represents a carbon-neutral and green solution producing a synthetic substitute of natural gas (SNG) which can be transported using the existing infrastructure for methane distribution.

The hydrogenation of CO<sub>2</sub> to produce methane, the Sabatier reaction, is an exothermic equilibrium process ( $\Delta H = -165 \text{ kJ mol}^{-1}$ ). Catalysts such as Ru, Ni, Fe, Co, or Rh, dispersed on oxide supports, are necessary to achieve satisfactory reaction rates and selectivity to CH<sub>4</sub> at low temperature. A common drawback of the Sabatier reaction is related to the formation of hot spots on the catalyst surface. These hot spots are responsible for lower performance due to the displacement of the thermodynamic equilibrium, which decreases selectivity related to the more favorable conditions for the occurrence of the endothermic Reverse Water Gas Shift. In addition, especially for Ni-based catalysts, irreversible deactivation due to Ni sintering can take place. To prevent significant catalyst overheating, highly thermoconductive supports can be used to promote easy heat dissipation, thus allowing suitable management of the exothermal effects.

Conventional ceramic supports such as alumina, silica, titania, etc. cannot assure an effective heat transfer, whereas silicon carbide (SiC) is reported to show high heat

conductivity and superior thermal stability [1–4]. To demonstrate the positive effect of SiC with respect to more insulating supports, Zhang et al. [2] compared the performance of nickel supported on SiC and Al<sub>2</sub>O<sub>3</sub> in CO methanation. They observed the sintering of Ni particles over Al<sub>2</sub>O<sub>3</sub> support and an increased carbon formation on the surface, which they attributed to the lower thermo-conductive properties of alumina with respect to SiC.

The rather low surface area of SiC and its chemical inertness represent features that strongly limit the direct dispersion of the active metal [1,4], and for this reason, the deposition of an intermediate high surface area mesoporous support is highly recommended. On the other hand, the deposition method of the support on the substrate represents a critical issue. Sun et al. [1] compared the performance in CO methanation of Ni/Al<sub>2</sub>O<sub>3</sub> catalysts deposited on SiC by EISA (evaporation-induced self-assembly), a method starting from aluminum isopropoxide, and DP (deposition-precipitation), a more traditional method starting from aluminum nitrate. The former technique provided a uniform and homogeneous alumina coating on SiC particles in contrast with the DP method, which generated Al<sub>2</sub>O<sub>3</sub> islands. This led to higher activity and selectivity to CH<sub>4</sub> in CO methanation of the catalyst prepared by the EISA method, also avoiding metal sintering and carbon deposition. Le et al. [3] also highlighted the importance of the preparation technique for Ni/SiC catalyst for the methanation of CO and CO<sub>2</sub>. They reported that the DP method, leading to good nickel dispersion, coupled with the high thermal conductivity of the support, gave better performance for both reactions. The DP method was also proposed by Jin et al. [4] for the preparation of Ni/Al<sub>2</sub>O<sub>3</sub>/SiC catalyst for CO methanation which led to a uniform dispersion of alumina on SiC and a good dispersion of Ni nanoparticles. The authors identified an optimal Al<sub>2</sub>O<sub>3</sub> loading providing the best catalytic performance.

All the above works were carried out in fixed bed reactors with particle catalysts; however, these show intrinsic limitations regarding radial heat transfer [5]. Therefore, structured catalysts have also been proposed, including ceramic or metal open-cell foams that offer distinctive advantages related to their high surface/volume ratio, low-pressure drops, radial mixing, and specifically outstanding mass and heat transfer [6,7]. In particular, highly conductive foams can improve the radial heat transport for non-adiabatic processes, e.g., for the CO<sub>2</sub> methanation on composite nickel foam catalysts [8]. Since the struts typically contain voids, the effective thermal conductivity is, however, below that of the pure solid material [5]. Frey et al. [9] compared three open-cell foams with the same morphology (consisting of SiC, alumina, and aluminum) and different intrinsic thermal conductivity to show the effect of heat transfer on the methanation reaction. The open-cell foams were coated with a ceria-zirconia layer followed by impregnation with Ni/Ru. Despite the highest thermal conductivity of aluminum, catalysts supported on this material showed a bad adhesion of the active phase. Consequently, SiC open-cell foams were the best compromise between the mechanical stability of the active layer and the thermal conductivity of the foamy substrate.

Similarly, Ricca et al. [10] investigated two structured substrates, made of SiC and aluminum, and shaped as honeycomb monolith and open-cell foam, respectively, whereby they deposited a washcoat layer of ceria-zirconia followed by Ni dispersion. The comparison with powder catalysts of the same composition highlighted that the better thermal distribution of the structured catalysts determined a flatter thermal profile. They found that this effect was more evident in the SiC monolith and also confirmed the bad adhesion of the active washcoat to the aluminum substrate already reported by Frey et al. [9]. In both works [9,10], a SiO<sub>2</sub> layer was generated on SiC substrate to better anchor the active phase. This is generally achieved by performing the thermal treatment of SiC under air. The oxidation of the SiC scaffold was used by Petersen et al. [11] to modify the thermal conductivity of β-SiC through the formation of an outer SiO<sub>2</sub> layer with a much lower thermal conductivity with an increasing thickness. The authors investigated Ru-based catalysts, showing a much higher activity at low temperature than their cheaper nickel counterparts, which is related to the easier reducibility of Ru [12]. The maximum fraction of SiO<sub>2</sub> explored caused a drop in the thermal conductivity of SiC/SiO<sub>2</sub> grains. As expected,

the selectivity to  $\text{CH}_4$  decreased with increasing the thickness of the  $\text{SiO}_2$  layer due to the worse heat transfer. As discussed, the quality of both dispersion and adhesion of the support to the structured substrate represents a critical matter, and the compromise between the formation of an oxide layer on the SiC surface decreasing the thermal conductivity but enhancing the adhesion of support must be carefully evaluated.

Santhosh et al. [13] produced polymer-derived (PD)  $\beta$ -SiC open-cell foams by impregnating polyurethane foam with a preceramic polymer and subsequent pyrolysis in an inert atmosphere (Ar) at 1200, 1500, and 1800 °C. They found that at 1200 °C, the foam struts consisted of a dense, non-stoichiometric, amorphous silicon carbide with oxygen impurities. Increasing the temperature to 1500 °C, oxygen was removed from the structure as CO, resulting in the formation of porous amorphous silicon carbide with excess carbon. Finally, pyrolysis at 1800 °C led to the crystallization of  $\beta$ -SiC and a corresponding increase in the thermal conductivity. It should be noted that these SiC foams, due to the inert atmosphere used in their processing, do not have any insulating  $\text{SiO}_2$  film at the surface. On one hand, this feature should be beneficial, since  $\text{SiO}_2$  limits the thermal exchange; on the other hand, it could result in a poorly bonded alumina washcoat.

In this work, polymer-derived SiC foams pyrolyzed at different temperatures were investigated as the substrate for a 3%Ru/ $\text{Al}_2\text{O}_3$  catalyst for  $\text{CO}_2$  hydrogenation to methane. Special attention was devoted to the deposition of the alumina-supported catalysts directly on the SiC foam substrates avoiding the formation of a further less conductive Si-oxide layer in between.

## 2. Results and Discussion

### 2.1. Characterization of Catalysts

The mechanical resistance of SiC foam disks prepared in this work is reported in Figure 1 in terms of the compressive strength as a function of the pyrolysis temperature. The compressive strength linearly increases up to a maximum of ca 1.3 MPa for a pyrolysis temperature of 1200 °C, and then it rapidly declines to reach a value below 0.1 MPa for those SiC foams treated at a temperature of 1800 °C.

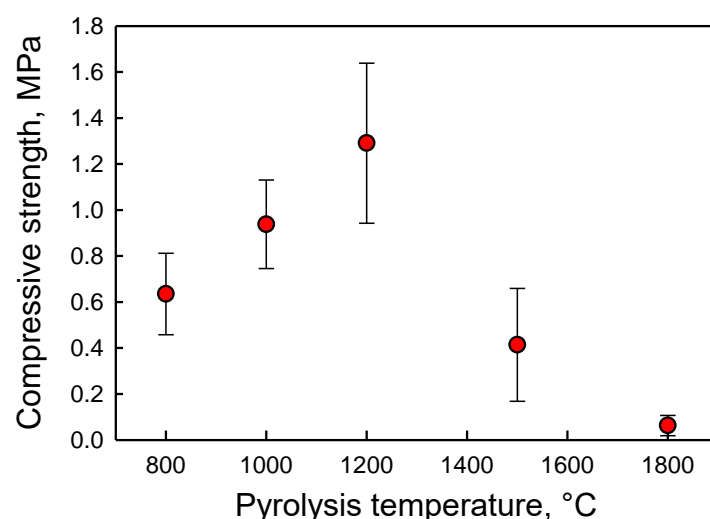


**Figure 1.** Compressive strength of the SiC foam disks as a function of the pyrolysis temperature.

Due to the brittleness of the F1800 disks, these samples easily lose fragments, especially during handling, deposition of the active catalytic layer as well as during loading into the quartz tube reactor for testing. This clearly appears when comparing images of the F1500- and F1800-based catalysts taken at different stages of preparation (Figure 2).

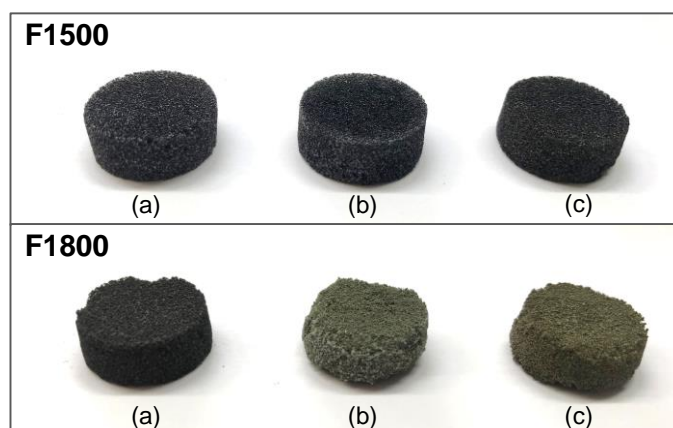


**Figure 2.** Images of F1500 (above) and F1800 (below) foam samples: (a) as pyrolyzed, (b) after the deposition of the  $\text{Al}_2\text{O}_3$  layer (by dip-coating), and (c) after the dispersion of Ru.

Figure 3 presents XRD results for the foam catalysts with the  $\text{Ru}/\text{Al}_2\text{O}_3$  active layer deposited on various SiC substrates. No significant modification of the XRD patterns was detected between Ru-impregnated and  $\text{H}_2$ -reduced catalysts; accordingly, data in Figure 3 generally refer to reduced catalysts but for RuA-F800 and RuA-F1000 samples that were only dried after impregnation with the Ru precursor. It was observed that the F800 and F1000 SiC substrates were mainly amorphous, whereas characteristic signals at  $2\theta$  angles around  $35.6$ ,  $60$ , and  $71.7^\circ$ , which are typical of the  $\beta$ -SiC phase, started to appear when the pyrolysis temperature reached  $1200^\circ\text{C}$  to eventually become very intense for the sample treated at  $1800^\circ\text{C}$ . Accordingly, the characteristic size of the  $\beta$ -SiC crystallites estimated by the Scherrer equation increased along with the pyrolysis temperature, passing from ca  $16$  to  $25$  Å and up ca  $580$  Å for samples based on F1200, F1500, and F1800 foams, respectively. The loss of mechanical strength occurring after pyrolysis at  $1500^\circ\text{C}$  seems to correlate with the porosity development [13], while the further drastic decrease of compressive strength at  $1800^\circ\text{C}$  seems to be due to the formation of large  $\beta$ -SiC crystallites.

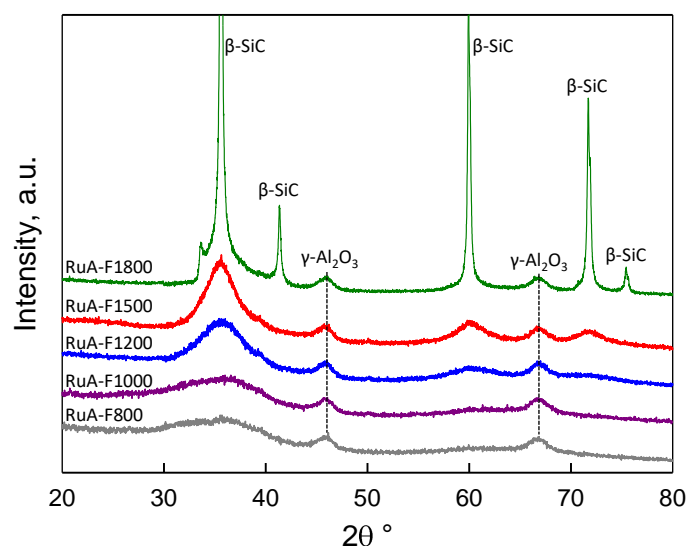


**Figure 3.** XRD patterns of RuA-F foam catalysts: RuA-F800 and -F1000 samples were only dried following impregnation with Ru; all other samples were further reduced in  $\text{H}_2$  at  $450^\circ\text{C}$ .

The formation of a  $\gamma$ - $\text{Al}_2\text{O}_3$  overlayer deposited on the foams by dip-coating and calcination of the pseudo-boehmite precursor was demonstrated by the characteristic broad signals at  $2\theta$  angles around  $45.9$  and  $66.7^\circ$ , from which a characteristic size of alumina crystallites was estimated constantly around  $60$  Å, regardless of the specific type of SiC

substrate. At variance, no evidence was found of the undesired formation of crystalline  $\text{SiO}_2$  due to the relatively low temperature of calcination which prevented SiC oxidation. This was also confirmed by the thermogravimetric analysis of the bare SiC substrates performed in air (not shown), excluding any significant weight change due to SiC oxidation up to 550 °C. Generally, no signals were detected in the XRD patterns of the structured catalysts relevant to Ru, which was due to the low loading of the noble metal and to its effective dispersion in the pores of the  $\gamma$ -alumina overlayer.

The SiC foams treated at increasing pyrolysis temperatures displayed similar geometrical features deriving from the PU template with open interconnected pores/cages of 400–500  $\mu\text{m}$  and dense triangular struts with a characteristic size of ca. 25  $\mu\text{m}$  (Figure 4). However, SEM analysis of bare foams showed a significant change in surface morphology, passing from a dense structure with a smooth texture characteristic of all samples treated up to 1500 °C (Figure 4a and its inset, Figure 4b), to a structure with some cracks and pores and a rough surface, covered with SiC crystals, typical of the sample treated at 1800 °C (Figure 4c and its inset).

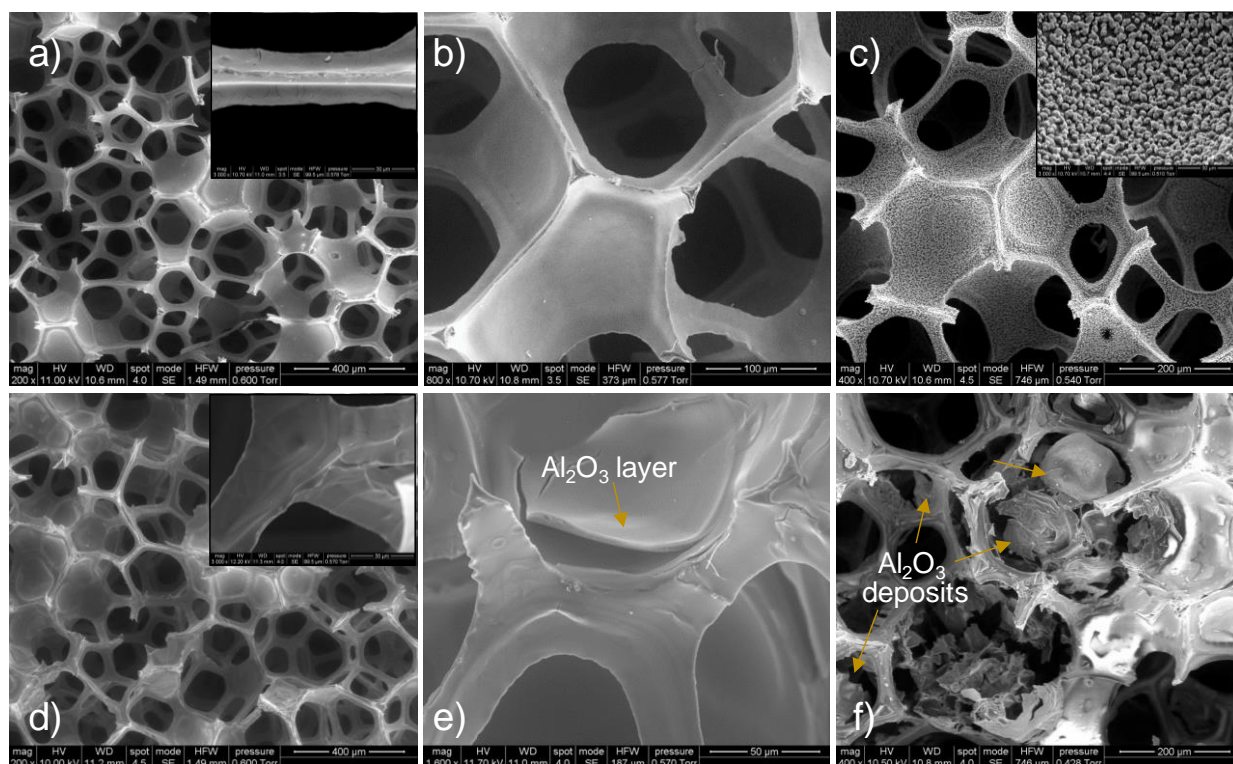


**Figure 4.** SEM images at different magnification showing the morphology of bare F1200 (a, and its inset), F1500 (b) and F1800 (c, and its inset) SiC foams supports as well as RuA-F1200 (d, and its inset); (e) and RuA(N)-F1200 (f) catalysts where an  $\text{Al}_2\text{O}_3$  overlayer was deposited by dip-coating or macropore filling, respectively.

As described in the Materials and Methods section, SiC foam disks were dip-coated with alumina starting from a pseudo-boehmite suspension representing the most conventional technique to washcoat honeycomb or foam monoliths. SEM micrographs of the final “activated” foam catalysts after  $\text{H}_2$ -reduction and catalytic methanation tests (Figure 4d and its inset; Figure 4e) showed that the dip-coating method produced a thin (2–3  $\mu\text{m}$ )  $\text{Al}_2\text{O}_3$  washcoat covering the SiC struts and cells rather uniformly so that the original morphology of the foams was preserved.

This suggests a good adhesion of alumina to the surface of SiC struts despite the absence of an intermediate  $\text{SiO}_2$  layer. Nevertheless, in some specific areas (i.e., closed windows), the alumina washcoat presented some cracks and/or was partially detached

from the SiC substrate (Figure 4e). A good dispersion of alumina was observed also for F1800, which was the only foam with a rough surface; SiC grains characterizing the surface of F1800 were still visible in the RuA-F1800 sample, though they were partially embedded in the alumina washcoat (not-shown).

At variance, the catalyst prepared by macropore filling of the SiC foam with aluminum nitrate solution showed (Figure 4f) a less uniform deposition of the resulting alumina loading, which mostly formed large grains entrapped in the cages and poorly anchored to the SiC struts.

Herein it is worth mentioning that the presence of a thin alumina overlayer (just few microns) applied on the SiC foam struts favors an easy penetration and uniform distribution of Ru throughout its whole depth. This is a significant advantage to avoid the common drawback of eggshell distribution and agglomeration of Ru nanoparticles that is often encountered in the preparation of supported catalysts using millimeter-sized alumina pellets or spheres [14,15]. This effect is due to the strong interaction of the Ru metal with the alumina inducing a fast precipitation of insoluble Ru-hydroxides that strongly limits the penetration depth of the precursor inside thick porous supports.

The  $N_2$  physisorption isotherms at 77K are presented in Figure 5 for RuA-F catalysts as well as for their corresponding SiC foam substrates. In agreement with previous results on similar SiC foams [13], the substrates obtained at temperatures up to 1200 °C showed flat isotherms with negligible adsorption volumes, typical of dense materials, which is also confirmed by SEM observations. As the pyrolysis temperature was further increased to 1500 °C and 1800 °C, the SiC foams progressively developed some (limited) mesoporosity, characterized by a wide distribution of pore sizes (Figure 5b), extending from ca 35 and up to 250 Å. Accordingly, the corresponding values of the BET specific surface area (Table 1) increased along with the temperature of pyrolysis up to ca 10 m<sup>2</sup>/g for the F1800 SiC foam sample.

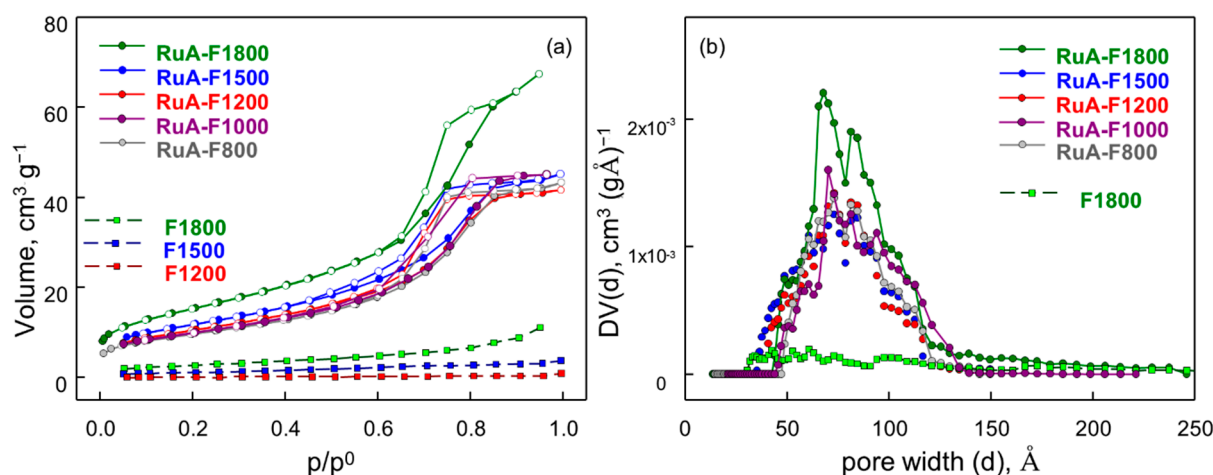


**Figure 5.**  $N_2$  adsorption (full symbols)/desorption (empty symbols) isotherms (a) and corresponding pore size distribution analysis (b) for selected RuA-Fxxxx reduced catalysts (circles) and their corresponding bare SiC foam substrates (squares).

The deposition of the alumina overlayer resulted in a significant increase in the adsorbed volumes and BET surface areas of the foam catalysts (Figure 5a, Table 1), which in turn depended on the actual loading of the oxide phase. In particular, regardless of the specific type of SiC foam substrate, the alumina washcoat was characterized by a relatively narrow pore size distribution in the range from 35 to 115 Å, with the highest frequency at ca. 70 and 80 Å.

**Table 1.** Geometric, compositional, and textural features of SiC foams and their corresponding RuA-Fxxxx catalysts after reduction.

Substrate	Apparent Density	Disk Volume	BET SiC	Al <sub>2</sub> O <sub>3</sub> Loading		Ru Loading	Ru on Al <sub>2</sub> O <sub>3</sub>	BET Catalyst	Pore Size (Mean)
	g cm <sup>-3</sup>	cm <sup>3</sup>	m <sup>2</sup> g <sup>-1</sup>	mg	% wt.	mg	%	m <sup>2</sup> g <sup>-1</sup>	Å
F800	0.16 ± 0.01	1.94	<0.5	82	20.9	2.8	3.4	34.2	72
F1000	0.17 ± 0.01	1.96	<0.5	86	20.5	2.8	3.3	35.3	72
F1200	0.17 ± 0.01	1.83	0.7	100	24.2	3.6	3.6	38.0	72
F1200	0.17 ± 0.01	1.83	0.7	100	24.2 *	2.7	2.7	8.7 *	50 *
F1500	0.15 ± 0.01	1.88	4.3	80	21.7	2.2	2.7	42.4	72
F1800	0.15 ± 0.01	1.58	9.8	77	26.5	2.3	3.0	55.4	69

\* Al<sub>2</sub>O<sub>3</sub> by macropore filling impregnation with an aqueous aluminum nitrate solution

Considering the nominal Al<sub>2</sub>O<sub>3</sub> loading on each foam sample, it was estimated that the BET specific surface area of the  $\gamma$ -alumina overlayer was constantly equal to  $170 \pm 10$  m<sup>2</sup>/g. The accuracy of this estimation was somehow limited by the error involved in the measurement of the actual Al<sub>2</sub>O<sub>3</sub> content for those samples having foam substrates with poor mechanical stability (F1500 and F1800).

Regarding the sample RuA(N)-F1200 prepared by the pore filling impregnation method, Table 1 shows that for an identical nominal oxide loading, the resulting BET surface area was only 8.7 m<sup>2</sup> g<sup>-1</sup>, indicating a much lower mesoporosity of the resulting alumina which was characterized by an average pore size around 50 Å and an estimated BET as low as 36 m<sup>2</sup> g<sup>-1</sup>. Accordingly, the XRD analysis of RuA(N)-F1200 (not shown) barely detected any characteristic signal  $\gamma$ -Al<sub>2</sub>O<sub>3</sub> suggesting an amorphous nature of the deposit obtained by this preparation method.

## 2.2. Catalytic CO<sub>2</sub> Methanation Tests

Given their superior mechanical features and relatively low processing temperatures, those RuA structured catalysts supported on SiC foams obtained at 1000 °C and 1200 °C were selected for testing in the catalytic methanation of CO<sub>2</sub>. Results are presented in Figure 6 in terms of the CO<sub>2</sub> conversion and CH<sub>4</sub> selectivity measured at the exit of the reactor as a function of the reaction temperature.

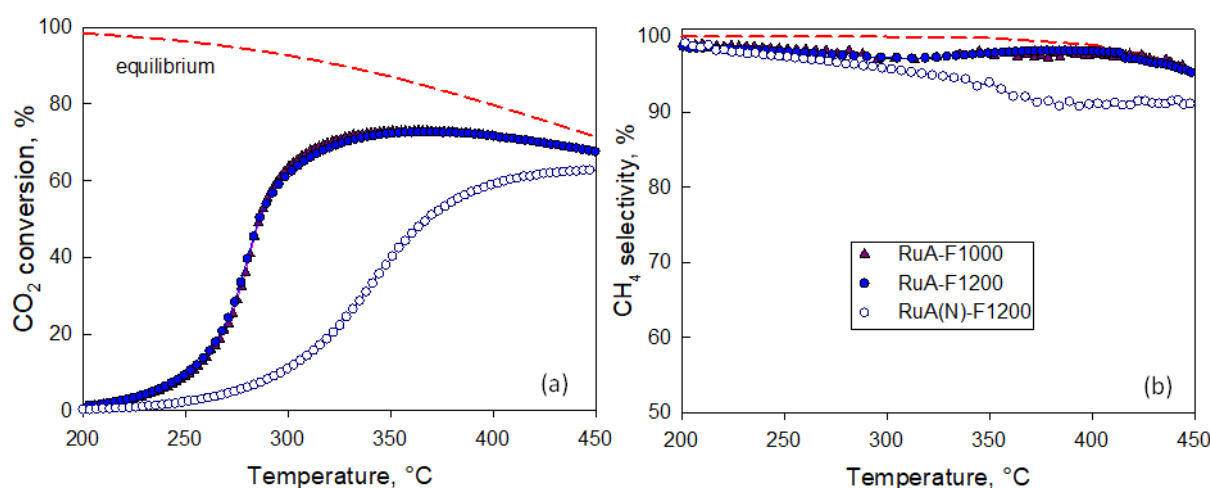


**Figure 6.** CO<sub>2</sub> conversion (a) and corresponding selectivity to CH<sub>4</sub> (b) as a function of the preheating temperature. The only other detected product of reaction was CO. Feed: CO<sub>2</sub>/H<sub>2</sub>/N<sub>2</sub> = 1/4/5. Red dashed lines represent thermodynamic equilibrium values (at constant T and P).

The characteristic conversion plots for RuA catalysts supported on either F1000 or F1200 SiC foams were superimposed, showing a typical S-shaped profile with an initial

slow rise followed by a steep increase above ca. 260 °C due to the light-off of the strong exothermic methanation reaction causing a significant temperature increase of the catalyst above the pre-heating level (up to ca 95 °C). Thereafter, beyond 400 °C, the CO<sub>2</sub> conversion started to approach the corresponding equilibrium values, slightly decreasing along with the reaction temperature. Both RuA-F catalysts converted CO<sub>2</sub> into methane with almost identical high selectivity values (constantly above 97%) once again approaching equilibrium for T > 380 °C and following the decreasing trend predicted by thermodynamic calculations due to the progressively larger formation of CO via the Reverse Water Gas Shift reaction which is favored at higher temperatures.

The RuA(N)-F1200 catalyst showed a qualitatively similar CO<sub>2</sub> conversion plot; however, this was shifted to higher temperatures by roughly 30 °C in the pre-ignition region, thus suggesting a lower overall intrinsic activity with respect to its RuA-F1200 counterpart. The process selectivity to methane was roughly unaffected in the low-to-mid conversion range up to 300 °C, i.e., where it is expected to be closely related to the intrinsic activity of the catalytic phase due to the prevailing of a kinetic regime. Beyond this point, CH<sub>4</sub> selectivity over RuA(N)-F1200 was slightly lower than that over the RuA-F1200 counterpart, which possibly suggests a worse heat management with the formation of localized hot-spot regions inside the catalytic disk at high conversion levels. In particular, the poor distribution of the active phase in the RuA(N)-F1200 sample, which was mostly trapped in the cells of the SiC foam, resulted in a poor contact with the conductive SiC struts (Figure 4f), thus favoring a local overheating and, in turn, promoting the undesired weakly endothermic Reverse Water Gas Shift reaction leading to the production of larger amounts of CO.

Additional methanation tests (not shown) were run over RuA-F1000 at fixed pre-heating (350 °C); the structured catalyst showed stable performance over a total of ca 7 h on stream while operating with a constant, self-sustained temperature as high as 440 °C recorded at its front (inlet) face. In turn, this confirmed the stability of the RuA active phase that was firmly anchored to the SiC foam support.

Figure 7a presents the Arrhenius plots derived from low-conversion data in Figure 6a which were acquired under pseudo-isothermal conditions and are representative of a pure kinetic regime. Coherently, all data points for each one of the tested catalysts follow a linear trend. The values of the apparent activation energy for the hydrogenation of CO<sub>2</sub> estimated by the slopes of the corresponding lines are very close to each other and equal to  $72.5 \pm 1.5 \text{ kJ mol}^{-1}$ . This is consistent with previously reported data over Ru/Al<sub>2</sub>O<sub>3</sub> [16–19] and suggests that all foam catalysts activate the same reaction mechanism regardless of the alumina deposition method as well as the type of the SiC support. Such a result was further confirmed by some additional tests (not shown) with RuA foam catalysts deposited over F1500 and F1800 SiC foams, always returning the same value of the apparent activation energy. Moreover, Figure 7a shows that the normalization of the CO<sub>2</sub> hydrogenation rate per unit mass of Ru in the catalysts' returned superimposed values for RuA-F1000 and RuA-F1200 samples. At variance, the RuA(N)-F1200 sample was characterized by a lower specific CO<sub>2</sub> hydrogenation activity, reduced by a factor of as much as 2.6. This is most probably due to the lower BET surface area and mesoporosity of the alumina layer causing a worse dispersion of the Ru metal nanoparticles.

Eventually, Figure 7b presents the results of the preliminary kinetic study on the apparent reaction order of the CO<sub>2</sub> hydrogenation (power law expression not accounting for the approach to equilibrium:  $R_w = k_w \cdot P_{\text{CO}_2}^n \cdot P_{\text{H}_2}^m$ ) which was conducted over the RuA-F1000 foam catalyst at fixed temperature and low conversion by varying the partial pressures of CO<sub>2</sub> and H<sub>2</sub> in the feed while keeping constant  $P_{\text{H}_2}$  and  $P_{\text{CO}_2}$ , respectively. In good agreement with previous literature reports on similar Ru/Al<sub>2</sub>O<sub>3</sub> catalysts [16,19], it was found that at low CO<sub>2</sub> conversion values the reaction rate has a dependence on H<sub>2</sub> partial pressure of ca 0.53 which is roughly 4 times stronger than on CO<sub>2</sub> (reaction order 0.14).

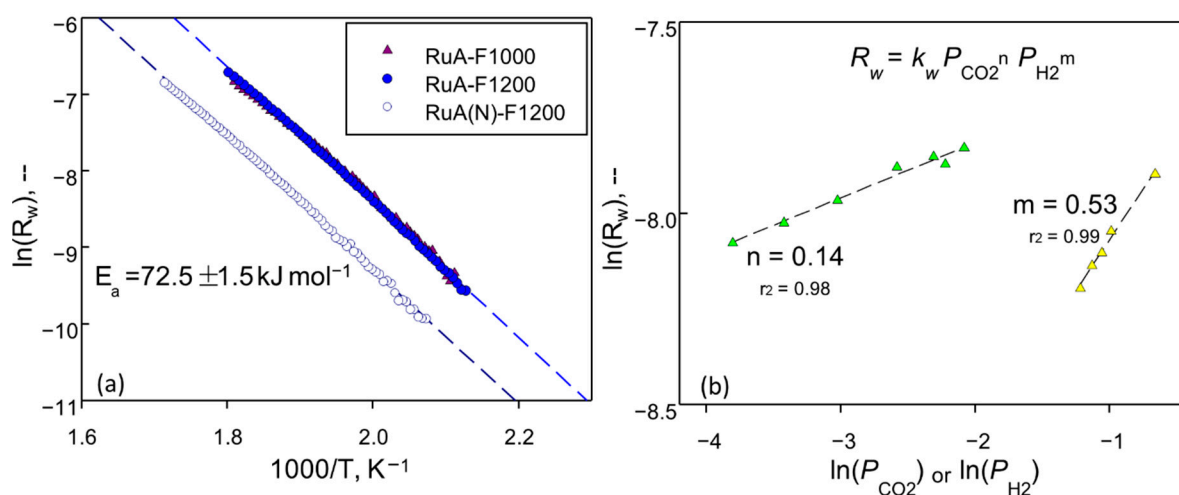


**Figure 7.** (a) Arrhenius plots for the catalytic hydrogenation of CO<sub>2</sub> over RuA-F1000, RuA-F1200, and RuA(N)-F1200 foam catalysts. (b) Effect of the partial pressure of CO<sub>2</sub> and H<sub>2</sub> on the catalytic hydrogenation rate at a fixed temperature (230 °C) over RuA-F1000 and corresponding apparent reaction orders.

### 3. Materials and Methods

#### 3.1. Preparation of SiC Foam Substrates

SiC foam disks (17–18 mm diameter, 7–7.8 mm height) were obtained by the replica method using flexible polyurethane (PU) PPI90 open cell foam (ARE- S.r.l, Rosate, Milan, Italy) following a published procedure [20]. PU templates were impregnated with polycarbosilane (SMP-10, Starfire Systems, Schenectady, USA) in acetone/hexane solution using a Pt catalyst (Platinum–divinyltetramethyldisiloxane complex in xylene, with Pt content of ~2%, Sigma–Aldrich, Saint Louis, MO, USA) and an SMP-10/PU weight ratio of 3. After drying at room temperature overnight, the impregnated foam samples were pyrolyzed under Ar (400 cc min<sup>-1</sup>) using a tubular alumina furnace (GERO, Neuhausen, Germany) within the temperature range of 800 °C–1500 °C. The samples were heated up to the maximum temperature at 5 °C min<sup>-1</sup> and were held for 1.5 h. The process also included an intermediate dwell of 0.5 h at 600 °C.

The samples processed at 1800 °C were pyrolyzed with the same conditions but using a graphite furnace (Astro Thermal Technology, Santa Barbara, CA, USA).

#### 3.2. Preparation of Catalysts

Catalysts were prepared by dip-coating the SiC substrates by immersion in a suspension of acid dispersible boehmite (Disperal–Sasol: 6.5 g in 43.2 mL of H<sub>2</sub>O and 0.3 g of HNO<sub>3</sub>, 65 wt%) followed by removal of excess suspension (by air-blowing). An alternative method of dispersion of the alumina support (macropore filling) was also implemented consisting of the immersion of the foam disks (pyrolyzed at 1200 °C) in an aqueous solution of Al(NO<sub>3</sub>)<sub>3</sub>·9H<sub>2</sub>O. Thereafter, all samples were dried at 120 °C and eventually calcined in air at 550 °C for 2 h. The deposition process was repeated to reach the final desired alumina loading on the foams (ca. 21–26% by weight).

Ruthenium was deposited by the incipient wetness impregnation method using a 1.4% wt. Ru(III) nitrosyl nitrate acidic solution (Merck, Darmstadt, Germany). The actual metal loading in the catalysts was estimated by the weight gain of the foam samples following impregnation and removal of the excess precursor solution with compressed air. The catalysts were then dried at 120 °C for 12 h and were finally reduced and activated in-situ at 450 °C under H<sub>2</sub>/N<sub>2</sub> flow before catalytic tests.

Foam catalysts were labeled as RuA-Fxxxx, where xxxx represents the pyrolysis temperature of the SiC substrate; the suffix (N) was added to the sample prepared by pore-filling with aluminum nitrate solution.

### 3.3. Characterization of Catalysts

The characterization of catalysts was generally performed on reduced samples unless otherwise stated.

The mechanical resistance of the foams pyrolyzed at different temperatures was evaluated by measuring their compressive strength with an MTS 810 (Material Test System, MTS system corp., Eden Prairie, Minnesota, USA) using a 5 kN load cell and cubic samples  $\sim (1.5 \times 1.5 \times 1.5) \text{ cm}^3$  at a displacement rate of  $1 \text{ mm min}^{-1}$ . At least four samples were measured for each pyrolysis temperature.

The morphology of the bare SiC foam substrates and their corresponding catalysts was inspected by scanning electron microscopy (SEM) with an FEI Inspect instrument (Thermo Fischer, Waltham, MA, USA).

X-ray diffraction (XRD) analysis of powdered samples was performed using a X'Pert PRO apparatus (Philips, Amsterdam, the Netherlands) with working radiation  $\text{CuK}\alpha$ , anti-scatter slit width: 7.5 mm, collecting patterns in the  $2\theta$  range  $20\text{--}80^\circ$ , scanning with a step size of  $0.013^\circ$  at  $0.156^\circ \text{ s}^{-1}$ .

Thermogravimetric analysis (TGA) of bare SiC foams was performed using a Netzsch STA 409 equipment (Netzsch Geraetebau GmbH, Selb, Germany). The 50 mg sample was loaded into an alumina crucible and heated in air flow ( $100 \text{ mL min}^{-1}$ ) at  $10^\circ \text{ C min}^{-1}$  up to  $550^\circ \text{ C}$  with 2 h holding at the maximum temperature.

$\text{N}_2$  adsorption measurements at 77 K were performed in an Autosorb 1-C (Quantachrome Instruments, Boynton Beach, FL, USA) after degassing samples at  $150^\circ \text{ C}$  for 3 h. The Brunauer, Emmett and Teller (BET) method and the Non-Linear Density Function Theory (NLDFT, cylindrical pore model) method were used to evaluate the specific surface area and the pore size distribution of the catalysts, respectively.

### 3.4. Catalytic $\text{CO}_2$ Methanation Tests

The catalytic methanation of gaseous  $\text{CO}_2$  was investigated in a fixed-bed quartz reactor with circular section ( $d_{in} = 20 \text{ mm}$ ,  $d_{out} = 25 \text{ mm}$ ) loaded with the foam disk. The reaction tests were run at atmospheric pressure in the temperature-programmed mode by heating up the catalysts from  $200$  to  $450^\circ \text{ C}$  with a rate of  $3^\circ \text{ C min}^{-1}$  under a flow of  $\text{CO}_2/\text{H}_2/\text{N}_2 = 1/4/5$  ( $20 \text{ SL/h}$ ). Reaction temperatures were measured by K-type thermocouples placed in contact with the front and back faces of the catalytic foam disk. Before testing, the catalysts were pre-reduced in situ at  $450^\circ \text{ C}$  under a flow of 20% vol.  $\text{H}_2/\text{N}_2$ .

The molar fractions of  $\text{CO}$ ,  $\text{CO}_2$ ,  $\text{CH}_4$ , and  $\text{H}_2$  in the product gas were measured by a continuous gas analyzer (Optima Advance, ABB, Zurich, Switzerland). Thereafter, the conversion of  $\text{CO}_2$  and the process selectivity to  $\text{CH}_4$  ( $s_{\text{CH}_4}$ ) were calculated according to the definitions:

$$x_{\text{CO}_2} = 100 \left( 1 - \frac{\text{CO}_2^{\text{out}}}{\text{CO}_2^{\text{out}} + \text{CH}_4^{\text{out}} + \text{CO}^{\text{out}}} \right) \quad (1)$$

$$s_{\text{CH}_4} = 100 \left( \frac{\text{CH}_4^{\text{out}}}{\text{CH}_4^{\text{out}} + \text{CO}^{\text{out}}} \right) \quad (2)$$

Gaseq software was used to calculate the equilibrium composition in the product gas at constant temperature and pressure. The rate of  $\text{CO}_2$  consumption per unit mass of Ru in the catalyst ( $R_w$ ) was estimated from low conversion data ( $<10\%$ ,  $\Delta T_{\text{out-in}} < 5^\circ \text{ C}$ ) by assuming an isothermal plug flow reactor operating under differential conditions with a constant molar flow rate according to the equation:

$$R_w \cong \frac{F_{\text{CO}_2} \cdot x_{\text{CO}_2}}{W_{\text{Ru}}} \left[ \text{mol g}_{\text{Ru}}^{-1} \text{ s}^{-1} \right] \quad (3)$$

where  $F_{\text{CO}_2}$  is the inlet molar flow of  $\text{CO}_2$  and  $W_{\text{Ru}}$  is the mass of Ru in the foam catalyst. The apparent activation energy of the catalytic  $\text{CO}_2$  hydrogenation was estimated by Arrhenius plots of  $R_w$ . The orders of reaction with respect to the partial pressure of

$\text{CO}_2$  and  $\text{H}_2$  were estimated by plots of  $\ln R_w$ , at a fixed temperature, vs.  $\ln P_{\text{CO}_2}$  and  $\ln P_{\text{H}_2}$ , respectively: the inlet molar ratio  $\text{H}_2/\text{CO}_2$  was varied in the range 2.9–4.9 for those experiments at constant  $P_{\text{CO}_2} = 0.1$  atm, and 3.1–15.7 for tests at constant  $P_{\text{H}_2} = 0.4$  atm.

#### 4. Conclusions

Polymer-derived SiC foam disks were prepared by a replica method using PPU open-cell foams (90 PPI) and were used as conductive, light-weight, structured substrates for a Ru/ $\text{Al}_2\text{O}_3$  catalyst for the hydrogenation of  $\text{CO}_2$  to methane. The formation of an insulating  $\text{SiO}_2$  layer on the surface of the SiC struts was prevented by a pyrolysis treatment under an inert atmosphere at temperatures varying from 800 to 1800 °C.

SiC foams obtained at 1000–1200 °C displaying an amorphous structure, a compact texture, and a compressive strength as high as 1.3 MPa were selected as viable substrates for the structured catalyst. Pyrolysis temperatures  $\geq 1500$  °C caused a significant loss of mechanical properties correlated with the porosity development and eventually, the formation of large  $\beta$ -SiC crystallites was observed at 1800 °C.

A quite uniform, well-anchored, thin  $\gamma$ - $\text{Al}_2\text{O}_3$  overlayer was formed on all SiC foam substrates by the dip-coating method with a pseudo-boehmite suspension. At variance, an alternative macro-pore filling method with an aqueous solution of aluminum nitrate precursor produced a poor dispersion of the resulting alumina, forming large deposits trapped in the foam cages. Eventually, the Ru active metal was dispersed on the  $\gamma$ - $\text{Al}_2\text{O}_3$  modified SiC foams by incipient wetness impregnation.

Catalytic methanation tests, performed in the temperature range from 200 to 450 °C in a fixed bed reactor, showed highly repeatable performance in terms of  $\text{CO}_2$  conversion as a function of temperature and, regardless of the specific type of SiC foam substrate, with high process selectivity to  $\text{CH}_4$  closely approaching equilibrium values in the whole temperature range explored.

Conversion data acquired under a pure kinetic-control regime suggested all Ru/ $\text{Al}_2\text{O}_3$ -SiC foam catalysts activated the same reaction mechanism regardless of the alumina deposition method. However, the catalyst prepared by the macropore-filling method provided worse catalytic performance due to the lower surface area of the alumina deposits reducing the dispersion of the active Ru metal. Moreover, the poor contact of the alumina with the conductive SiC foam substrate was also responsible for the larger formation of CO at high temperatures, related to the occurrence of localized hot spots in the structured catalyst favoring the undesired Reverse Water Gas Shift reaction.

**Author Contributions:** Conceptualization, S.C., L.L. and G.D.S.; investigation, E.M.C., M.B. and B.S.; data curation, E.M.C., M.B., and B.S.; writing—original draft preparation, L.L.; writing—review and editing, S.C. and G.D.S.; visualization, S.C.; supervision, S.C., L.L. and G.D.S.; funding acquisition, L.L., and G.D.S. All authors have read and agreed to the published version of the manuscript.

**Funding:** This research was funded by Ministero Università e Ricerca—Italy (PRIN 2017PMR932, “Nanostructured Porous Ceramics for Environmental and Energy Applications”).

**Institutional Review Board Statement:** Not applicable.

**Informed Consent Statement:** Not applicable.

**Data Availability Statement:** The data presented in this study are available on request from the corresponding authors.

**Acknowledgments:** The authors wish to gratefully acknowledge Luciano Cortese for the SEM characterization.

**Conflicts of Interest:** The authors declare no conflict of interest.

## References

1. Sun, J.; Feng, Q.; Liu, Q.; Ji, S.; Fang, Y.; Peng, X.; Wang, Z.-j. An Al<sub>2</sub>O<sub>3</sub>-Coated SiC-Supported Ni Catalyst with Enhanced Activity and Improved Stability for Production of Synthetic Natural Gas. *Ind. Eng. Chem. Res.* **2018**, *57*, 14899–14909. [[CrossRef](#)]
2. Zhang, G.; Suna, T.; Penga, J.; Wang, S.; Wang, S. A comparison of Ni/SiC and Ni/Al<sub>2</sub>O<sub>3</sub> catalyzed total methanation for production of synthetic natural gas. *Appl. Catal. A Gen.* **2013**, *462–463*, 75–81. [[CrossRef](#)]
3. Le, T.A.; Kang, J.K.; Park, E.D. CO and CO<sub>2</sub> Methanation Over Ni/SiC and Ni/SiO<sub>2</sub> Catalysts. *Top. Catal.* **2018**, *61*, 1537–1544. [[CrossRef](#)]
4. Jin, G.; Gu, F.; Liu, Q.; Wang, X.; Jia, L.; Xu, G.; Zhong, Z.; Su, F. Highly stable Ni/SiC catalyst modified by Al<sub>2</sub>O<sub>3</sub> for CO methanation reaction. *RSC Adv.* **2016**, *6*, 9631–9639. [[CrossRef](#)]
5. Wehinger, G.D. Improving the radial heat transport and heat distribution in catalytic gas-solid reactors. *Chem. Eng. Proc. Process Intensif.* **2022**, *177*, 108996. [[CrossRef](#)]
6. Giani, L.; Groppi, G.; Tronconi, E. Mass-Transfer Characterization of Metallic Foams as Supports for Structured Catalysts. *Ind. Eng. Chem. Res.* **2005**, *44*, 4993–5002. [[CrossRef](#)]
7. Hetsroni, G.; Gurevich, M.; Rozenblit, R. Metal foam heat sink for transmission window. *Int. J. Heat Mass Transf.* **2005**, *48*, 3793–3803. [[CrossRef](#)]
8. Cimino, S.; Cepollaro, E.M.; Lisi, L.; Fasolin, S.; Musiani, M.; Vázquez-Gómez, L. Ru/Ce/Ni Metal Foams as Structured Catalysts for the Methanation of CO<sub>2</sub>. *Catalysts* **2021**, *11*, 13. [[CrossRef](#)]
9. Frey, M.; Romero, T.; Roger, A.-C.; Edouard, D. Open cell foam catalysts for CO<sub>2</sub> methanation: Presentation of coating procedures and in situ exothermicity reaction study by infrared thermography. *Catal. Today* **2016**, *273*, 83–90.
10. Ricca, A.; Truda, L.; Palma, V. Study of the role of chemical support and structured carrier on the CO<sub>2</sub> methanation reaction. *Chem. Eng. J.* **2019**, *377*, 120461.
11. Petersen, E.M.; Rao, R.G.; Brandon, C.; Vance, B.C.; Tessonier, J.-P. SiO<sub>2</sub>/SiC supports with tailored thermal conductivity to reveal the effect of surface temperature on Ru-catalyzed CO<sub>2</sub> methanation. *Appl. Catal. B Environ.* **2021**, *286*, 119904.
12. Cimino, S.; Russo, R.; Lisi, L. Insights into the cyclic CO<sub>2</sub> capture and catalytic methanation over highly performing Li-Ru/Al<sub>2</sub>O<sub>3</sub> dual function materials. *Chem. Eng. J.* **2022**, *428*, 131275.
13. Santhosh, B.; Ionescu, E.; Andreolli, F.; Biesuz, M.; Reitz, A.; Albert, B.; Sorarù, G.D. Effect of pyrolysis temperature on the microstructure and thermal conductivity of polymer-derived monolithic and porous SiC ceramics. *J. Eur. Ceram. Soc.* **2021**, *41*, 1151–1162. [[CrossRef](#)]
14. Porta, A.; Falbo, L.; Visconti, C.G.; Lietti, L.; Bassano, C.; Deiana, P. Synthesis of Ru-based catalysts for CO<sub>2</sub> methanation and experimental assessment of intraporous transport limitations. *Catal. Today* **2020**, *343*, 38–47. [[CrossRef](#)]
15. Apuzzo, J.; Cimino, S.; Lisi, L. Ni or Ru supported on MgO/ $\gamma$ -Al<sub>2</sub>O<sub>3</sub> pellets for the catalytic conversion of ethanol into butanol. *RSC Adv.* **2018**, *8*, 25846–25855. [[CrossRef](#)] [[PubMed](#)]
16. Wang, X.; Hong, Y.; Shi, H.; Szanyi, J. Kinetic modeling and transient DRIFTS-MS studies of CO<sub>2</sub> methanation over Ru/Al<sub>2</sub>O<sub>3</sub> catalysts. *J. Catal.* **2016**, *343*, 185–195. [[CrossRef](#)]
17. Dreyer, J.A.H.; Li, P.; Zhang, L.; Beh, G.K.; Zhang, R.; Sit, T.W.Y. Influence of the oxide support reducibility on the CO<sub>2</sub> methanation over Ru-based catalysts. *Appl. Catal. B Environ.* **2017**, *219*, 715–726.
18. Cimino, S.; Boccia, F.; Lisi, L. Effect of alkali promoters (Li, Na, K) on the performance of Ru/Al<sub>2</sub>O<sub>3</sub> catalysts for CO<sub>2</sub> capture and hydrogenation to methane. *J. CO<sub>2</sub> Util.* **2020**, *37*, 195–203.
19. Falbo, L.; Visconti, C.G.; Lietti, L.; Szanyi, J. The effect of CO on CO<sub>2</sub> methanation over Ru/Al<sub>2</sub>O<sub>3</sub> catalysts: A combined steady-state reactivity and transient DRIFT spectroscopy study. *Appl. Catal. B Env.* **2019**, *256*, 117791.
20. Jana, P.; Zera, E.; Sorarù, G.D. Processing of preceramic polymer to low density silicon carbide foam. *Mater. Des.* **2017**, *116*, 278–286.